ADVANCED HEALTHCARE MATERIALS
www.advhealthmat.de

# Monitoring of Cell Layer Integrity with a Current-Driven Organic Electrochemical Transistor

*Leona V. Lingstedt, Matteo Ghittorelli, Maximilian Brückner, Jonas Reinholz, N. Irina Crăciun, Fabrizio Torricelli, Volker Mailänder, Paschalis Gkoupidenis, and Paul W. M. Blom**

**The integrity of CaCo-2 cell barriers is investigated by organic electrochemical transistors (OECTs) in a current-driven configuration. Ion transport through cellular barriers via the paracellular pathway is modulated by tight junctions between adjacent cells. Rupturing its integrity by $H_2O_2$ is monitored by the change of the output voltage in the transfer characteristics. It is demonstrated that by operating the OECT in a current-driven configuration, the sensitive and temporal resolution for monitoring the cell barrier integrity is strongly enhanced as compared to the OECT transient response measurement. As a result, current-driven OECTs are useful tools to assess dynamic and critical changes in tight junctions, relevant for clinical applications as drug targeting and screening.**

Epithelial and endothelial barriers of the human body act as the major obstacle for ions and small molecules to the bloodstream, as such "invaders" cannot easily diffuse across the cell layer.[1] As the epithelium consists of a packed monolayer of cells, it provides a physical barrier to separate the organism from the external environment,[1] and several transport routes within this barrier exist.[1,2] Besides the transcellular pathway, the paracellular pathway is limited by specialized complexes between adjacent cells, including the tight junctions.[1,2] Tight junctions consist of complexes of transmembrane and cytoplasmic proteins and are located at the apical domain of neighboring epithelial cells regulating the paracellular passage of ions and small molecules (**Figure 1**).[2] These transport routes within these barriers can be exploited for drug delivery for instance.[1,2] In the body, a number of different barriers are present differing from each other by the tightness of the paracellular barrier.[2] The brain capillaries and the skin epithelium represent the tightest barrier tissues in the body, while colon and stomach are of intermediate tightness.[2] The lower parts of the small intestine are determined as the leaky epithelial tissue due to different expression of proteins. This allows or blocks different ions, resulting in an increased ion flux.[2] Hence, the small intestine is considered as the major place for drug absorptions,[2] but is also vulnerable to attack by pathogenic organisms and compounds.[3–5] One possible way of disruption is targeting the tight junctions or other junctions between adjacent cells as shown in Figure 1.[1,3] Loss or dysfunction of tight junctions would lead to an uncontrolled passage of ions, macromolecules, and other cells through the barrier, which might disrupt uptake of nutrients and electrolytes and harm the body.[3] Hence, the state of the cell barrier integrity acts as a precursor to dysfunction and disease, and can be used for a model for toxicological studies.[3–5] Furthermore, it can be exploited for drug delivery and drug targeting, as in the last decades the safe and reversible opening of these junctions for a controlled drug absorption and penetration has been thoroughly studied.[1,2] An efficient method for barrier tissue characterization will help to conceive models for a better understanding of how epithelial and endothelial barriers work; and how to use this knowledge in drug testing and drug targeting, aiming among others for the replacement for animal testing in toxicological profiling.[1,3]

The tightness of the intercellular junctional complex is reflected on the transepithelial electrical resistance (TEER), measuring the paracellular ion flow.[1–3] TEER can be measured with an epithelial Volt-Ohm meter.[3] This measurement is easy to perform but suffers from slow temporal resolution and reproducibility.[3,6] A more optimized approach is the use of impedance spectroscopy to measure the resistance (= TEER) and capacitance ($c_d$) of the cell layer.[7,8] Other traditional techniques to assess the integrity of the cellular barrier are immunofluorescence and permeability assay.[2,6] The organic electrochemical transistors (OECT) provides a unique platform for the integration of electronics and biological systems.[9] With the ability to conduct both electronic and ionic carriers, OECTs play a complementary role in health care and biomedical diagnostics.[9,10] The applications of OECTs range from electrophysiological

Dr. L. V. Lingstedt, M. Brückner, Dr. J. Reinholz, Dr. N. I. Crăciun, Prof. V. Mailänder, Dr. P. Gkoupidenis, Prof. P. W. M. Blom
Max Planck Institute for Polymer Research
Ackermannweg 10, 55128 Mainz, Germany
E-mail: blom@mpip-mainz.mpg.de
Dr. M. Ghittorelli, Dr. F. Torricelli
Department of Information Engineering
University of Brescia
Via Branze 38, 25123 Brescia, Italy
M. Brückner, Dr. J. Reinholz, Prof. V. Mailänder
Dermatology Clinic
University Medical Center of the Johannes Gutenberg-University, Mainz
Langenbeckstr. 1, 55131 Mainz, Germany
The ORCID identification number(s) for the author(s) of this article can be found under https://doi.org/10.1002/adhm.201900128.



**DOI: 10.1002/adhm.201900128**

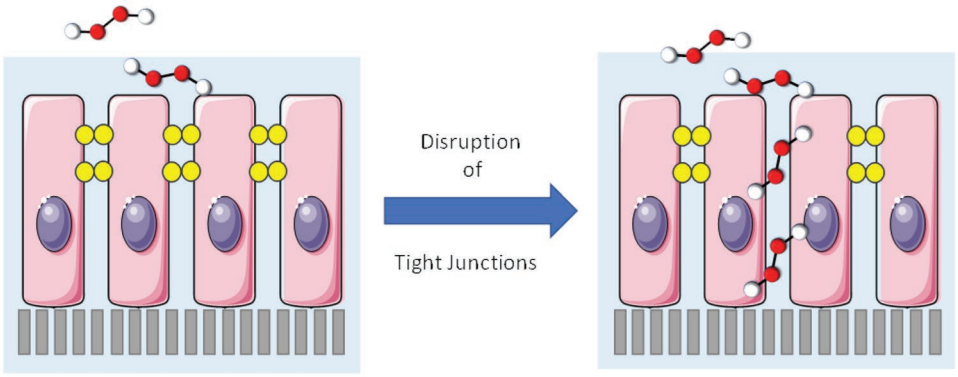


**Figure 1.** Cartoon of a packed layer of epithelial cells, connected by tight junctions (depicted in yellow). Tight junctions disruption can be the result of toxins, here symbolized by hydrogen peroxide. Cartoon has been created by images of SMART.[25]

recordings of organs in terms of electrically active tissues, to biosensing applications, as in the detection of electrolytes and metabolites or integration with cells.[9,11–13] In particular, using the OECT for assessing cell barrier integrity has been proven to be an attractive method in comparison to traditional techniques.[3,6,14,15] By integrating the OECT with epithelial cells, minute variations in paracellular ion flow, caused by toxic compounds, has been detected.[4,5,14] A further enhancement of the sensitivity level of the OECTs would enable real-time detection of the integrity of tight junctions during disease and treatment. It has been recently shown that the sensitivity in ion detection of aqueous electrolytes can be further enhanced and reaching the highest value ever reported so far for ion-sensitive transistors by using the OECT in the current-driven configuration.[16]

Here, we show the integration of epithelial cells with the OECT in the current-driven configuration to further enhance the sensitivity in monitoring the cell barrier integrity. The process of incorporating a healthy cell layer and rupturing its integrity by $H_2O_2$, has been monitored by the change of the output voltage in the transfer characteristics. For sensitivity, different peroxide concentrations have been used to evaluate the effect on the transfer characteristics as well as on the response times, in reference to the earlier stated OECT transient response method. Our approach has been optimized to allow higher sensitivity in direct comparison, emphasizing the OECT as a competitive measuring tool for cell barrier assessment in respect to the conventional methods.

The OECT device structure with an integrated cell layer is shown in **Figure 2**a and assembles the typical 3-terminal transistor configuration of source, drain, and gate. In the current-driven OECT, the device is connected in series with a current generator, as illustrated in Figure 2b.[16,17] The input voltage $V_{in}$ is applied at the gate and in reference to the standard OECT configuration the new topology gives $V_{in} = V_G$ enabling the control of the channel doping. The output voltage $V_{out}$ is measured at the drain ($V_{out} = V_D$).[16] By using the current generator, we force a current bias $I_B$ ($I_B = I_D$), and as a result we measure $V_{out}$.[16] Thus, the configuration can also be described as a voltage divider of the supply voltage $V_{DD}$ of the transistor.[18] Figure 2c shows typical transfer characteristics ($V_{out}$–$V_{in}$) of a current-driven OECT for a series of $I_B$. By applying a negative $V_{in}$ (e.g., $V_{in} = -V_{DD} = -0.2$ V), PEDOT:PSS is still highly doped, resulting in a small output resistance $r_o$ of the channel. Because of $V_{out} = V_{DD} - I_B \cdot r_o$, $V_{out}$ is close to $+V_{DD}$. By increasing $V_{in}$,

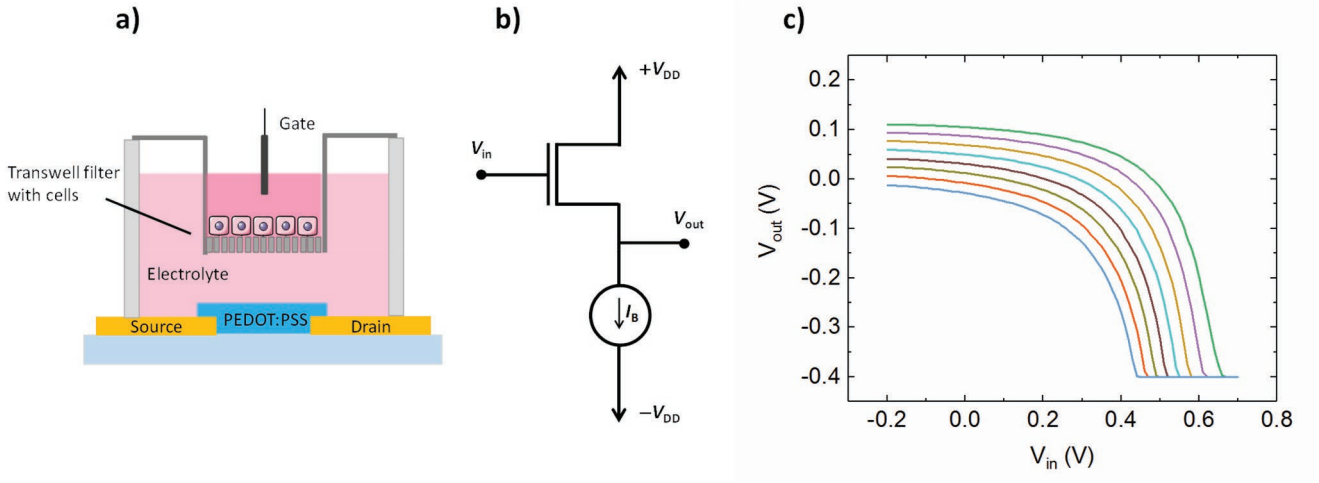


**Figure 2.** OECT as a sensor for cell barrier integrity: a) Device structure with an integrated Transwell filter with cells.[25] b) Schematic circuit of the current-driven configuration. c) Measured transfer characteristics of a current-driven OECT for $I_B$ ranging from –0.7 till –1.4 mA (top to bottom) at $V_{DD} = 0.2$ V. Device dimension were $W = 2$ mm, $L = 1$ mm. A Ag/AgCl gate electrode and EMEM cell culture medium as an electrolyte was used.

cations are injected into the channel, dedope it and $r_o$ increases. Consequently, $V_{out}$ lowers and the OECT, operating in the linear regime, eventually changes to the saturation regime. The transition from linear to saturation regime, takes place when $V_{in} - V_{out} = V_P$, where $V_P$ is the pinch-off voltage. At saturation, the channel close to the drain electrode is nearly completely dedoped and $I_D$ is almost independent of $V_D$. $r_o$ significantly increases and $V_{out}$ approaches the minimum supply voltage of $-V_{DD}$. The sharp modulation of $V_{out}$ is illustrated in Figure 2c for $I_B$ ranging from –0.7 to –1.4 mA for a supply voltage of $V_{DD}$ = 0.2 V. The minimum supply voltage of –0.4 V is limited by the voltage compliance of the current generator.

Here, we demonstrate the OECT in the current-driven configuration as a sensor for cell layer integrity using the Caco-2 cell line, a well-known model for the gastrointestinal barrier.[14,19] Incorporating a cell layer between the gate and the channel creates a barrier for passing ions that impedes the ion flow.[3] **Figure 3**a shows the integration of an intact layer of cells, which are tightly connected by tight junctions (depicted in yellow). This causes a shift of the ($V_{out}$–$V_{in}$)-transfer curve toward higher $V_{out}$. The high cell resistance $r_{cell}$ (=TEER) induces a low ionic flux and consequently higher $V_{in}$ are needed to dedope the channel. Reactive oxygen species are known for their irreversible effect on barrier tissue integrity. Excessive reactive oxygen species lead to tissue injuries in form of inflammation or loss of intestinal barrier functions. This may mediate phosphorylation and regulation of tight junction protein–protein interactions.[1,6] Thus, the addition of toxic compounds in the form of hydrogen peroxide ($H_2O_2$), indirectly damages the tight junctions and finally leads to a cell layer opening:[3,6] TEER decreases and thereby lowers $V_{out}$, pulling the ($V_{out}$–$V_{in}$)-curve toward the starting condition, meaning the absence of cells (Figure 3a). A more detailed view on the process of the cell layer opening is shown in Figure S1 in the Supporting Information with intermediate measurements in the Supporting Information. For a better cell viability cell culture medium was used as the electrolyte.[19] Adding an aqueous $H_2O_2$ solution dilutes the cell culture medium, meaning changing the electrolyte's concentration and so its resistance $r_{med}$. The current-driven OECT is highly sensitive to changes in the ion concentration, thus a very small shift of the ($V_{out}$–$V_{in}$)-transfer curve according to the change in the switching voltage is observed in Figure 3b.[16] Noting, that we define the switching voltage as the minimum $V_{in}$ required to operate the OECT in saturation. No further shift over a period of 60 min is observed (Figure 3b), therefore this configuration is a reliable measuring method for assessing the cell barrier integrity.

State-of-art OECT-based methods for the cell barrier function evaluation have been proposed by Owens and coworkers.[3,14] More in detail, an approach operates the OECT in the time domain and the measurement of the tissue integrity is demonstrated.[3] The other approach operates the OECT in the frequency domain and cell coverage and differentiation is demonstrated. Both these methods are based on the OECT transient response. Here we benchmark the current-driven OECT method for cell integrity evaluation by comparing it with the method proposed by Owens and coworkers in 2012.[3] In this, work the transient response of the OECT was measured by pulsing $V_G$. Integrating the OECT with epithelial cells changes

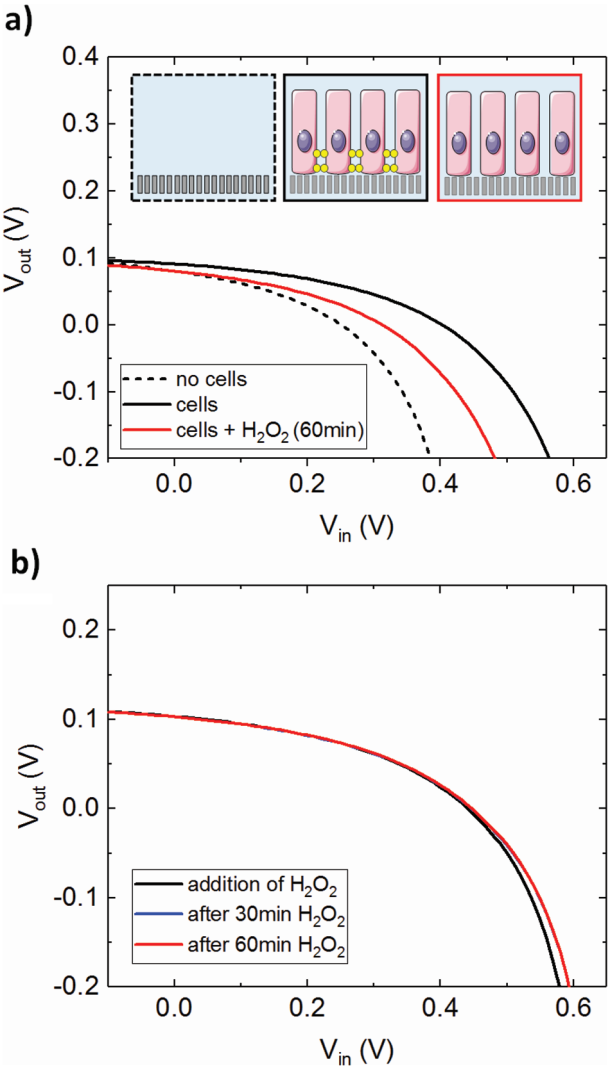


**Figure 3.** Transfer characteristics of the current-driven configurated OECT monitoring the addition of $1 \times 10^{-3}$ M $H_2O_2$ a) in the presence and b) absence of epithelial cells (control experiment) at $V_{DD}$ = 0.2 V and $I_B$ = –1.6 mA. The inset in panel (a) shows the Transwell filter in the absence of a cell layer (black dashed frame), a healthy cell layer with tight junctions (yellow, black frame), and a ruptured cell layer (red frame). The inset has been created by images of SMART.[25] Device dimension were $W$ = 2 mm, $L$ = 1 mm. A Ag/AgCl gate electrode and EMEM cell culture medium as an electrolyte was used.

the paracellular ion flow and this has been affecting the speed of the transistor response till it reaches steady state, in the end resembled in the transient response. By using toxic compounds, the integrity of cellular barriers has been detected.[3] Hence, both methods were conducted using the same devices under the same conditions. **Figure 4**b demonstrates the cell layer disruption by using a rather high concentration of $5 \times 10^{-3}$ M $H_2O_2$ using the current-driven OECT: as shown before a significant shift of the ($V_{out}$–$V_{in}$)-transfer curve is seen when the cell layer is integrated. An almost completely opening of the cell layer is achieved with $H_2O_2$, as the initial state of the characteristic curve is nearly reached after 60 min. In the reference method, the transient response is measured. In this time, the channel

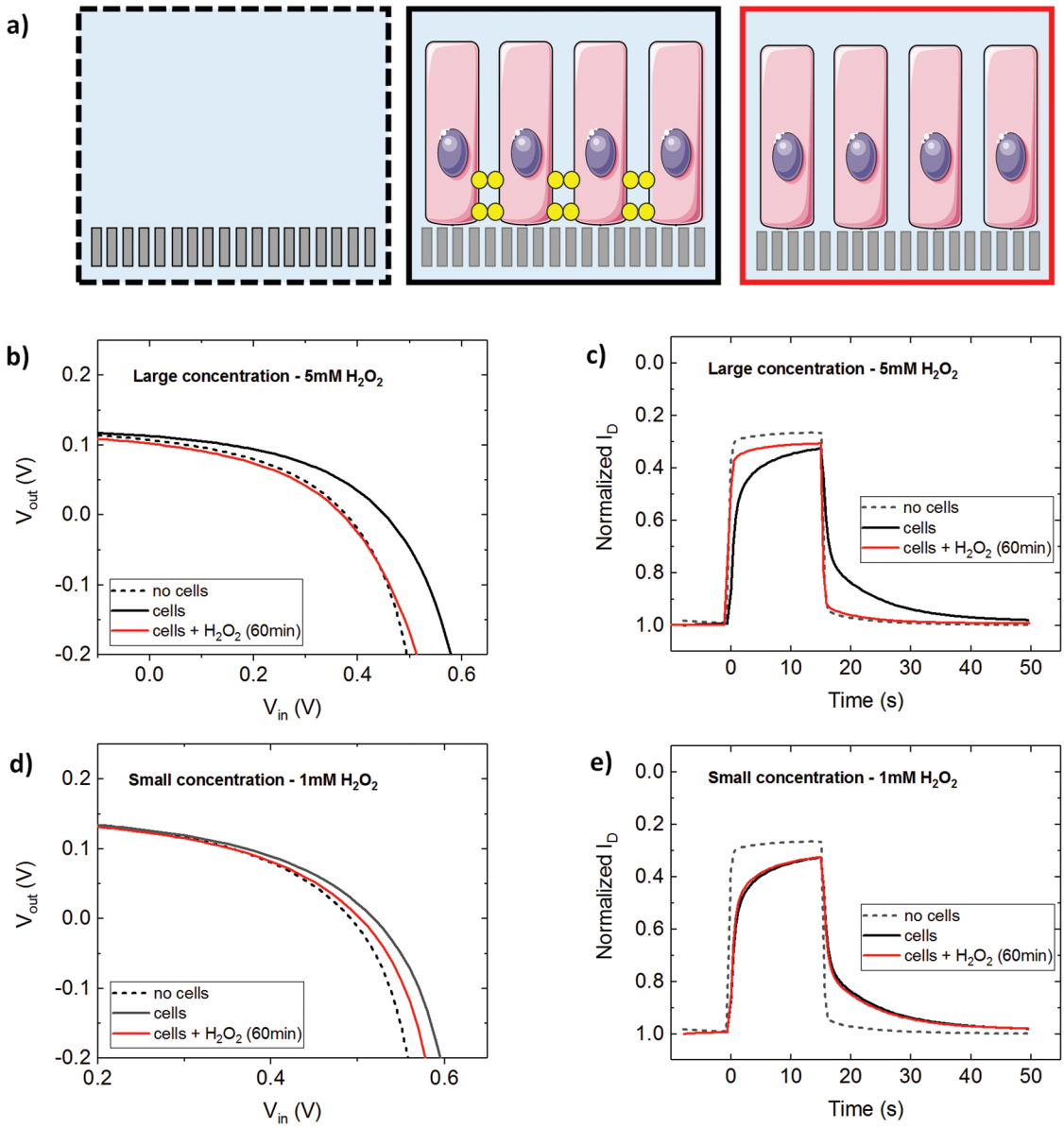


**Figure 4.** OECT as a cell barrier integrity sensor for $H_2O_2$: a) shows the Transwell filter in the absence of a cell layer (black dashed frame) and the condition of the cell layer (black and red frame). The integrity of the cellular barrier is symbolized by the presence and absence of tight junctions (yellow). The OECT response in the b) current-driven and c) in the standard configuration in the absence and presence of cells adding $5 \times 10^{-3}$ M $H_2O_2$. The transfer characteristics in the current-driven configuration with and without cells adding $1 \times 10^{-3}$ M $H_2O_2$ is shown in d), while the analogues transient response in the reference method is seen in e). The inset has been created by images of SMART.[25] Transfer characteristics were conducted at $V_{DD} = 0.2$ V and $I_B = -1.1$ mA b) and –0.6 mA c) in the current-driven configuration, while $V_D = -0.1$ V was used in the standard configuration. Device dimension were $W = 2$ mm, $L = 1$ mm. A Ag/AgCl gate electrode and EMEM cell culture medium as an electrolyte was used.

is dedoped, resembled in a modulation of $I_D$ in Figure 4c. The integration of a cell layer decreases the ion flux, in other words slows down the transistor response till it reaches steady state. A smaller modulation of $I_D$ in the same pulse duration as before is the result (Figure 4c). Adding $H_2O_2$ in a concentration of $5 \times 10^{-3}$ M increases again the ion flow through the membrane, and therefore the modulation of $I_D$, reaching toward the initial modulation in the absence of cells. Figure 4d,e shows the results for a lower concentration of $1 \times 10^{-3}$ M $H_2O_2$. While a smaller but still detectable shift in the ($V_{out}$–$V_{in}$)-transfer curve is obtained with the current-driven OECT, no changes are visible with the reference method. Control experiments with $H_2O_2$ were carried out to confirm that no damage of the reactive oxygen species has occurred with neither the gate electrode nor the conductive polymer (Figure S2, Supporting Information).

In the current-driven OECT, we defined the characteristic response by $V_{in}$ at $V_{out} = -0.2$ V in small time intervals. For the reference method, the response time or the time constant of the system was defined by fitting the output current $I_D$ with a two exponential decay function (mathematical derivation is

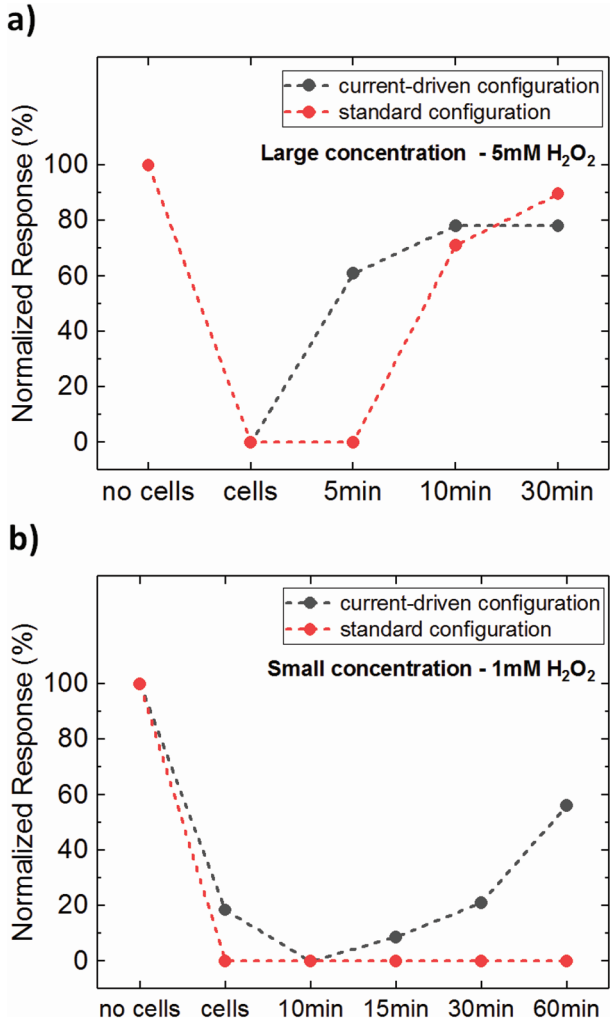


**Figure 5.** The corresponding normalized response of the OECT in the standard (response time of the OECT) and current-driven configuration (shift of input voltage $V_{in}$) after the addition of $H_2O_2$ for a) $5 \times 10^{-3}$ M) and b) $1 \times 10^{-3}$ M. The response in the standard configuration is defined as the time constant of the output current $I_D$. The response of the current-driven OECT is defined by the shift of $V_{in}$ at $V_{out} = -0.2$ V, while the dielectric relaxation time is used for the transient response in the reference method. The transfer characterisics were taken at $V_{DD} = 0.2$ V and $I_B = -1.1$ mA a) and $-0.6$ mA b) in the current-driven configuration, while $V_D = -0.1$ V was used in the standard configuration. Device dimension were $W = 2$ mm, $L = 1$ mm. A Ag/AgCl gate electrode and EMEM cell culture medium as an electrolyte was used.

described in Figure S3 in the Supporting Information). For both techniques, the extracted responses were normalized for comparison purposes.

For the higher concentration ($5 \times 10^{-3}$ M $H_2O_2$) a cell barrier rupture is observed in both cases, revealing an abrupt cell opening. This is quantified as a change of 80-90% of the normalized device response (**Figure 5**a). While the current-driven configuration shows already after 5 min a significant effect of 60% by adding $H_2O_2$ and reaching after only 10 min a steady state of 80% ruptured layer, the reference method shows a delay of 10 min before reaching after 30 min the final state of 90% cell opening (Figure 5a). For lower concentration ($1 \times 10^{-3}$ M $H_2O_2$), this picture completely changes. While in the reference method no change is detected, two concurrently processes can be detected in the current-driven configuration. Due to the slow cell opening process, the dilution of the electrolyte is eventually revealed. Increasing the electrolyte's resistance, higher $V_{in}$ are needed to dedope the channel, leading to a shift of the ($V_{out}$–$V_{in}$)-curve to the right. This is resembled by a decreased normalized response. After 10 min, the rupture of the tight junctions slowly progresses. Destroying the tight junctions and decreasing TEER, it affects the ($V_{out}$–$V_{in}$)-curves by continually shifting to the left. In Figure 5b, this is expressed by an increasing normalized response, eventually reaching 60% cell opening, highlighting the partial cell opening. Overall, for low $H_2O_2$ concentrations no detectable change in response time is observed, while lower concentrations emphasize the higher sensitivity achieved in the current-driven configuration. This improved sensitivity could be explained by noting that the sensitivity of current-driven OECTs depends on the main device parameters, namely the pinch-off voltage $V_P$ and the current prefactor $\beta$[16]

$$S = \Delta VSW/\Delta c = \Delta V_P/\Delta c + K\,\Delta\beta/\Delta c \quad (1)$$

where $K = (I_B/\beta^3)^{1/2}/2$ and $I_B$ is the bias current.

When using the current-driven OECT configuration for measuring the cell barrier, the number of cations that at a given gate voltage drift inside (dedoping) or outside (doping) the polymeric channel of the OECT depends on the cell barrier integrity. As a consequence, the cell barrier integrity affects both $V_P$ and $\beta$ and according with Equation (1) both these variations are reflected in the sensitivity. In addition, Equation (1) suggests that sensitivity can be further improved by increasing $I_B$, which is an additional design variable. In the case of the standard configuration, the sensitivity depends on the transient time of ions drifting inside or outside the polymer and the drain current is normalized. As a consequence, the information about the amount of ions gating the OECT is lost. Moreover, since the transient response method is sensitive to the transient time of ions, it is expected that the sensitivity increases by reducing the distance between the OECT and the cell barrier. Unfortunately, this condition is difficult to achieve in practice, because of the Transwell filter used for the membrane suspension. The OECTs measurement were amended by simple TEER measurements by a handheld epithelial Volt-Ohm meter. Figure S4 in the Supporting Information states overall the same trend in the normalized response for both cases.

It should be noted that one requirement for using the reference OECT method as a sensor for cell barrier integrity is the need to increase the effective cell layer resistance of the Transwell filter.[3,20] Expressed in an equivalent circuit, the integration of a cell layer is represented in an additional resistor $R_{cell}$ (=TEER) and capacitor $C_{cell}$ in parallel, which are connected in series with the capacitor of the channel $C_{CP}$ and the resistor of the electrolyte medium $R_{med}$.[3,20] By decreasing the cell filter area with polydimethylsiloxane (PDMS), the effective cell layer resistance can be increased. In this way, the change in resistance caused by the cell layer disruption is amplified and after all detectable. This requirement is not necessary for the current-driven configuration as shown in Figure S5 in the

Supporting Information. Modifying the cell filter with PDMS is time consuming, causes a higher risk for contamination and errors, and thus lowers reproducibility. Overall, the current-driven configuration not only enhances the sensitivity with higher temporal resolution than the reference method, but also has advantages in terms of fabrication and execution in measuring the barrier integrity.

Tight junctions are of dynamic nature, changing and adjusting their structure rapidly according to physiological stimuli. Thus conventional measurement techniques have been limited by their invasive, elaborate, and slow method.[3,6] That is why the key advantage of the OECT is the ability to dynamically assess the barrier properties in a very sensitive matter and depth.[3] Providing a label-free and noninvasive detection of toxic compound and pathogens, OECTs are believed to have a strong potential for toxicological purposes and clinical applications.[3,9,21] The reversible opening of epithelial tight junctions and enhancing paracellular permeation by tight junction-modulators (e.g., chitosan) have been shown great potential in improving drug delivery.[1,2] Conventional methods like immunofluorescence staining and microscopic TEM have successfully yielded detailed structural information but are strongly limited by temporal resolution.[2,6] OECT would offer a fast and sensitive way to monitor cellular barrier dynamics, which could promote in combination with other measurement technologies the understanding and optimization of tight junction-modulators and how to exploit them for disease therapies and drug delivery.

In summary, OECTs have been shown as suitable sensors for cell barrier integrity, differentiating from other traditional techniques due to their low cost, temporal resolution, and sensitivity. Using the OECT in the current-driven configuration has already demonstrated to have the highest sensitivity in ion detection at low voltages. Here, by combining the current-driven transistor configuration with an integrated cell layer, has indeed achieved higher sensitivity and temporal resolution in detecting disruption in barrier function. The process of the cell opening can be detected in detail as a variation of the output voltage. We believe that by tuning the device toward greater sensitivity, this method will have high potential for fundamental research, as well as applications in biosensing. The current-driven OECT is a useful method to assess dynamic and critical changes in tight junctions, achieving a depth of information, useful for clinical applications as drug targeting and screening.

## Experimental Section

*Cell Culture*: Caco-2 cells were seeded at $1.5 \times 10^5$ cells/insert on Transwell filters (1.12 $cm^2$, 0.4 µm) and cultured in EMEM (Eagle's Minimum Essential Medium, Invitrogen) with 10% FBS (fetal bovine serum, Invitrogen), $2 \times 10^{-3}$ M glutamine (GlutaMax-1, 100X, Invitrogen) and Pen-strep (10 000 U $mL^{-1}$ penicillin, 10 000 µg $mL^{-1}$ streptomycin, Invitrogen) at 37 °C in a humidified atmosphere with 5% $CO_2$ with a medium change every few days. The cell filters were used after 14 days in culture, providing a high TEER of 500–700 Ω $cm^2$.[3,19,22] The cells already reached confluency after only 3–4 days, but it was the differentiation of further structures and polarization that resulted in high TEER values, needed for the experiments. Additional confocal laser scanning microscopic images (cLSM) of immunofluorescently stained Caco-2 cells against the tight junction protein occoludin confirmed confluency and the presence of tight junctions (Figure S6, Supporting Information). For this, cells were cultivated for 15 days on a Transwell collagen permeable support 3.0 µm PTFE membrane, 12 mm insert from Corning. The cells were fixed with 4% paraformaldehyde in Dulbecco's phosphate buffered saline (PBS) for 10 min at room temperature, followed by permeabilization with 0.2% Triton-X 100 in PBS. Staining was performed with occludin monoclonal antibody (clone: OC-3F10, FITC conjugated, Thermo # 33-1511), with a concentration of 5 µg $mL^{-1}$ in 250 µL PBS for 2 h at 4 °C in the fridge. Experiments were conducted on the LSM SP5 STED Leica Laser Scanning Confocal Microscope (Leica, Germany), composed of an inverse fluorescence microscope DMI 6000CS equipped with a multilaser combination using a HCX IRAPO L $25.0 \times 0.95$ water objective. The specimen's FITC dye was excited with the excitation laser 488 nm and detected with an emission filter at 510–550 nm. For an increased cell layer resistance, the area was reduced to ≈0.08 $cm^2$ by applying PDMS on the back side for the filter. For the PDMS-modified Transwell filters, an additional collagen coating according to literature was implemented for improved cell attachment.[23]

*Device Fabrication*: Source and drain gold contacts were thermally evaporated using a shadow mask for defined channel dimensions ($W$ = 2 mm, $L$ = 1 mm). In advance, a chromium layer was evaporated for a better adhesion. PEDOT:PSS (Hereaus, Clevios PH1000) was used as the conductive channel material. Zonyl (FSO- 100, Du Pont) acting as a surfactant was added to the PEDO:PSS dispersion for a better film formation. For an enhanced conductivity, dimethyl sulfoxide (DMSO) was added in a volume ratio of 10%. Spin coating conditions defined the layer thickness of ≈100 nm. A final annealing of 1 h at 140 °C was implemented after film deposition.[24] A polymethyl methacrylate (PMMA)-well was placed on top for a defined volume of the electrolyte, using double-sided tape to prevent leakage. The devices were rinsed in DI water before measurements.

*Device Measurements*: All electrical measurements were performed in ambient atmosphere by using a Keithley 4200-Semiconductor Characterization System and analyzed by using OriginLab software. Cell culture medium (EMEM) was used as an electrolyte in the Transwell filter as well as in the well. A Ag/AgCl electrode (pellet, 2 mm, Warner Instruments) was used as a gate, immersed in the Transwell filter. The operating gate voltage was kept well below 1.0 V to avoid water electrolysis and any cell damage. The measurements were conducted at ambient conditions as the cell layers were stable for at least 90 min at ambient temperature (Figure S7, Supporting Information).[4,5] The Transwell filter remained the entire measurement time on the device at room temperature to avoid any changes or disturbances in the setup. The hydrogen peroxide was added to the apical side of the cell filter in the concentration of $1 \times 10^{-3}$ and $5 \times 10^{-3}$ M (volume change below 5%). By repeated pipetting up and down, the solution was thoroughly mixed. The TEER was measured with a handheld Volt-Ohm meter EVOM$^2$ from World Precision Instruments.

For the transfer characteristics in the current-driven configuration, the supply voltage was $V_{DD}$ = 0.2 V and the input voltage $V_{in}$, applied at the gate, was swept from –0.2 to –0.65 V at a specific current bias $I_B$. The normalized response was obtained by $\Delta I_D/I_0$, which is the change of the drain current by applying a gate voltage, divided by the drain current when $V_{in}$ is off.

In the reference measurements, the transient response was measured by pulsing the gate voltage $V_G$ at 300 mV for 20 s at a drain voltage $V_D$ = –0.1 V. The response time was determined by the Fourier Transform of the multiexponential decay of the experimental transient response. The normalized response was calculated analogue to $I_D$ by $\Delta\tau/\tau_0$.

*Statistical Analysis*: Preprocessing data: For the data analysis, Fourier Transformation and normalization were used; Sample size: Five device samples were used for the analysis, each consisting of an array of three transistors with the dimension of $W$ = 2 mm and $L$ = 1 mm. Before each cell experiment, the transistor was tested for operational stability. For each peroxide concentration (1 and $5 \times 10^{-3}$ M), the experiment was repeated with three different cell filters with and without PDMS modification. Each experiment was performed in the standard and

current-driven OECT configuration; Data presentation: The data is presented as one set of experiment. Additional experiments were designed for reproducibility. Among all measurements, the overall behavior (electrical characterization) was reproducible; Software: For the statistical analysis, Microsoft Excel and OriginLab were used.

## Supporting Information

Supporting Information is available from the Wiley Online Library or from the author.

## Conflict of Interest

The authors declare no conflict of interest.

## Keywords

bioelectronics, cell barriers, inverters, organic electrochemical transistors, toxicology

Received: January 28, 2019
Revised: July 1, 2019
Published online:

[1] M. A. Deli, *Biochim. Biophys. Acta, Biomembr.* **2009**, *1788*, 892.
[2] K. Sonaje, E.-Y. Chuang, K.-J. Lin, T.-C. Yen, F.-Y. Su, M. T. Tseng, H.-W. Sung, *Mol. Pharmaceutics* **2012**, *9*, 1271.
[3] L. H. Jimison, S. A. Tria, D. Khodagholy, M. Gurfinkel, E. Lanzarini, A. Hama, G. G. Malliaras, R. M. Owens, *Adv. Mater.* **2012**, *24*, 5919.
[4] S. Tria, L. Jimison, A. Hama, M. Bongo, R. M. Owens, *Biosensors* **2013**, *3*, 44.
[5] S. A. Tria, M. Ramuz, L. H. Jimison, A. Hama, R. M. Owens, *J. Visualized Exp.* **2014**, *84*, e51102.
[6] S. A. Tria, L. H. Jimison, A. Hama, M. Bongo, R. M. Owens, *Biochim. Biophys. Acta, Gen. Subj.* **2013**, *1830*, 4381.
[7] J. Wegener, D. Abrams, W. Willenbrink, H.-J. Galla, A. Janshoff, *BioTechniques* **2004**, *37*, 590.
[8] J. Wegener, C. R. Keese, I. Giaever, *Exp. Cell Res.* **2000**, *259*, 158.
[9] J. Rivnay, S. Inal, A. Salleo, R. M. Owens, M. Berggren, G. G. Malliaras, *Nat. Rev. Mater.* **2018**, *3*, 17086.
[10] J. Rivnay, S. Inal, B. A. Collins, M. Sessolo, E. Stavrinidou, X. Strakosas, C. Tassone, D. M. Delongchamp, G. G. Malliaras, *Nat. Commun.* **2016**, *7*, 11287.
[11] a) M. Braendlein, A.-M. Pappa, M. Ferro, A. Lopresti, C. Acquaviva, E. Mamessier, G. G. Malliaras, R. M. Owens, *Adv. Mater.* **2017**, *29*, 1605744; b) A.-M. Pappa, V. F. Curto, M. Braendlein, X. Strakosas, M. J. Donahue, M. Fiocchi, G. G. Malliaras, R. M. Owens, *Adv. Healthcare Mater.* **2016**, *5*, 2295; c) P. Lin, X. Luo, I.-M. Hsing, F. Yan, *Adv. Mater.* **2011**, *23*, 4035; d) M. Sessolo, J. Rivnay, E. Bandiello, G. G. Malliaras, H. J. Bolink, *Adv. Mater.* **2014**, *26*, 4803; e) J. Rivnay, H. Wang, L. Fenno, K. Deisseroth, G. G. Malliaras, *Sci. Adv.* **2017**, *3*, e1601649.
[12] P. Lin, F. Yan, J. Yu, H. L. W. Chan, M. Yang, *Adv. Mater.* **2010**, *22*, 3655.
[13] N. Wang, A. Yang, Y. Fu, Y. Li, F. Yan, *Acc. Chem. Res.* **2019**, *52*, 277.
[14] M. Ramuz, A. Hama, J. Rivnay, P. Leleux, R. M. Owens, *J. Mater. Chem. B* **2015**, *3*, 5971.
[15] M. Ramuz, A. Hama, M. Huerta, J. Rivnay, P. Leleux, R. M. Owens, *Adv. Mater.* **2014**, *26*, 7083.
[16] M. Ghittorelli, L. Lingstedt, P. Romele, N. I. Crăciun, Z. M. Kovács-Vajna, P. W. M. Blom, F. Torricelli, *Nat. Commun.* **2018**, *9*, 1441.
[17] X. Wu, A. Surendran, J. Ko, O. Filonik, E. M. Herzig, P. Müller-Buschbaum, W. L. Leong, *Adv. Mater.* **2019**, *31*, e1805544.
[18] M. Braendlein, T. Lonjaret, P. Leleux, J.-M. Badier, G. G. Malliaras, *Adv. Sci. (Weinheim, Ger.)* **2017**, *4*, 1600247.
[19] D. A. Volpe, *J. Pharm. Sci.* **2008**, *97*, 712.
[20] G. C. Faria, D. T. Duong, A. Salleo, C. A. Polyzoidis, S. Logothetidis, J. Rivnay, R. Owens, G. G. Malliaras, *MRS Commun.* **2014**, *4*, 189.
[21] P. Leleux, J. Rivnay, T. Lonjaret, J.-M. Badier, C. Bénar, T. Hervé, P. Chauvel, G. G. Malliaras, *Adv. Healthcare Mater.* **2015**, *4*, 142.
[22] J. Reinholz, C. Diesler, S. Schöttler, M. Kokkinopoulou, S. Ritz, K. Landfester, V. Mailänder, *Acta Biomater.* **2018**, *71*, 432.
[23] G. Sitterley, *BioFiles* **2008**, *3.8*, 5.
[24] L. V. Lingstedt, M. Ghittorelli, H. Lu, D. Koutsouras, T. Marszalek, F. Torricelli, N. I. Crăciun, P. Gkoupidenis, P. W. M. Blom, *Adv. Electron. Mater.* **2019**, *26*, 1800804.
[25] Servier Medical Art by Servier, licensed under a Creative Commons Attribution 3.0 Unported License, https://creativecommons.org/licenses/by/3.0/ (accessed: February 2019).